Princeton Plasma Physics Laboratory

PPPL-

PPPL-
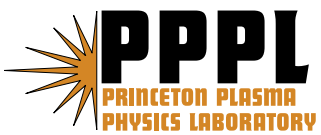
PPPL
PRINCETON PLASMA PHYSICS LABORATORY

Princeton Plasma Physics Laboratory
Report Disclaimers

Full Legal Disclaimer

Trademark Disclaimer

PPPL Report Availability

Princeton Plasma Physics Laboratory:

http://www.pppl.gov/techreports.cfm

Office of Scientific and Technical Information (OSTI):

http://www.osti.gov/bridge

Related Links:

U.S. Department of Energy

Office of Scientific and Technical Information

Fusion Links

First observation of ELM pacing with vertical jogs in a spherical torus

S.P. Gerhardt[1], **J-W. Ahn**[2], **J.M. Canik**[2], **R. Maingi**[2], **R. Bell**[1],
D. Gates[1], **R. Goldston**[1], **R. Hawryluk**[1], **B.P. Le Blanc**[1],
J. Menard[1], **A.C. Sontag**[2], **S. Sabbagh**[3] and **K. Tritz**[4]

[1] Princeton Plasma Physics Laboratory, Princeton, NJ, USA
[2] Oak Ridge National Laboratory, Oak Ridge, TN, USA
[3] Columbia University, New York, NY, USA
[4] The Johns Hopkins University, Baltimore, Maryland, USA

Abstract

Experiments in a number of conventional aspect ratio tokamaks have been successful in pacing edge localized modes (ELMs) by rapid vertical jogging of the plasma. This paper demonstrates the first pacing of ELMs in a spherical torus plasma. Applied 30 Hz vertical jogs synchronized the ELMs with the upward motion of the plasma. 45 Hz jogs also lead to an increase in the ELM frequency, though the synchronization of the ELMs and jogs was unclear. A reduction in the ELM energy was observed at the higher driven ELM frequencies.

(Some figures in this article are in colour only in the electronic version)

1. Introduction

The standard operating scenario for most shaped tokamaks involves a regime with steep gradients in the plasma temperature and density just inside the separatrix [1]. This high-confinement regime is typically known as an H-mode. Because the gradients inside the core plasma are believed to be limited by turbulence (except in regimes with additional internal transport barriers), the height of this H-mode edge pedestal, as parametrized by the values of plasma density and temperature at the inner edge of the steep gradient region, plays a key role in determining the overall fusion performance of a tokamak [2]. Furthermore, the high pressure at the plasma boundary serves to broaden the pressure profile, enhancing the ideal global stability of the configuration [3, 4], as well as providing non-inductive current drive through the gradient-driven bootstrap current [5–7]. For these reasons, the baseline scenario in the International Thermonuclear Experimental Reactor (ITER) is H-mode.

However, the good confinement properties of the H-mode pedestal are often interrupted by brief expulsions of particles and energy, known as edge localized modes (ELMs) [8–11]. A commonly accepted model for the ELM cycle comes from the theory of coupled peeling–ballooning modes [12, 13]. After each ELM, the pressure gradient and the resulting current (including the bootstrap current) are relaxed. The pressure gradient then evolves back towards the pre-ELM state on the timescale of the confinement time, while the current gradient evolves on the longer current diffusion time. At some point, either the pressure gradient or the edge current evolves to a state unstable to peeling (kink) and/or ballooning modes, an ELM occurs, and the cycle repeats. The resulting impulsive heat load provides a severe test to the materials in the divertor, and can limit their useful lifetime if the ELM sizes are too large [14–17].

A number of techniques have been proposed to solve this transient heat loading problem. These include (i) eliminating the ELMs entirely in regimes where another mechanism takes the role of flushing impurities and regulating the pedestal pressure (ii) developing regimes with natural small and frequent ELMs or (iii) dramatically reducing the ELM size by increasing their frequency via external perturbations of some sort. With regard to option (i), ELM-free regimes with minimal impurity accumulation have been observed when resonant magnetic perturbations (RMPs) are applied in DIII-D [18–20]. The 3D fields degraded the transport sufficiently for the pedestal to no longer be unstable to the MHD modes that drive ELMs [18]. Internal coils are now proposed for ITER in order to apply these fields. An attractive ELM-free regime known as the quiescent H-mode has been developed in DIII-D [21], where the pedestal pressure is regulated by a steady saturated instability known as the edge harmonic oscillation (EHO) [21, 22]. This configuration was then replicated in ASDEX-Upgrade [23] and JET [24] and a similar regime

has been observed in JT-60 [25]. The enhanced D$_\alpha$ regime demonstrated in Alcator C-MOD relies on quasi-coherent MHD near the separatrix to regulate the pedestal [26]; this is similar to the forced density rise scenario [27] found in PDX. Small ELM regimes include the type III [8, 28] and type V ELMs [29]. Among techniques to increase the ELM frequency, ELM pacing via rapid pellet injection has been demonstrated in ASDEX-Upgrade [30, 31] and JET [31, 32], and is among the preferred methods for ITER [17]. ELM pacing by pulsed 3D fields has been developed in NSTX [33, 34].

An additional method for pacing ELMs is to apply rapid vertical jogs to the plasma. This method was first demonstrated in TCV [35], and subsequently developed in ASDEX-Upgrade [36] and JET [37–39]. In these cases, the radial-field (vertical position control) systems are used to rapidly move the plasma up and down by a small fraction of the minor radius. This motion is observed to trigger ELMs at a rate more rapid than the intrinsic ELM frequency, leading to smaller ELMs.

It is the purpose of this paper to report the first observation of ELM triggering and pacing via vertical position jogs in a spherical torus (ST) plasma. These results demonstrate that pacing via jogs can be implemented in an ST, despite the improved pedestal stability at low aspect ratio [40], and may provide an alternative to magnetic ELM pacing techniques [33, 34]. These results also provide further evidence that this pacing technique can be used without internal coils or vacuum chambers with high toroidal resistance.

The organization of this paper is as follows. Section 2 provides some background information, while section 3 describes the techniques used to induce rapid vertical jogs in the NSTX plasma. The material in section 4 demonstrates the triggering and pacing of ELMs with vertical jogs and a discussion and summary are given in section 5.

2. Experimental background

NSTX [41] is a medium size ST, designed to test the predicted advantageous confinement and stability properties of the ST [42]. It has a major radius of $R = 0.85$ m, and typically operates at aspect ratios $R/a = 1.3$–1.4 (here, R is the major radius of the plasma and a is the minor radius, defined as half the distance between the inboard and outboard plasma boundaries at the midplane). H-mode access is routine [43–45], and a wide variety of ELM types have been reported, from the small ELM type-V regime [29] to type-1 and 'giant' ELMs [45, 46].

Typical plasma boundary shapes for this study, as well as the vessel, coils and a few important diagnostics, are shown in figure 1. PPPU2 and PPPL2 are names of axisymmetric poloidal flux loops, whose flux and voltage signals are used to assess and control the plasma vertical position and velocity [47]. The chords labelled USXR (ultra-soft x-ray) and Bol. (bolometer) are three of the 30 chords of the horizontal USXR detection system [48]. These detectors can be run without filters in bolometry mode, or with beryllium filters of variable thickness, changeable on a shot-to-shot basis. The three boundary shapes in the figure will be discussed in section 4.

The discharges described in this study came from two sets. Both sets have on-axis toroidal field strengths of $B_T = 0.45$ T, injected neutral beam powers of 6 MW and lower
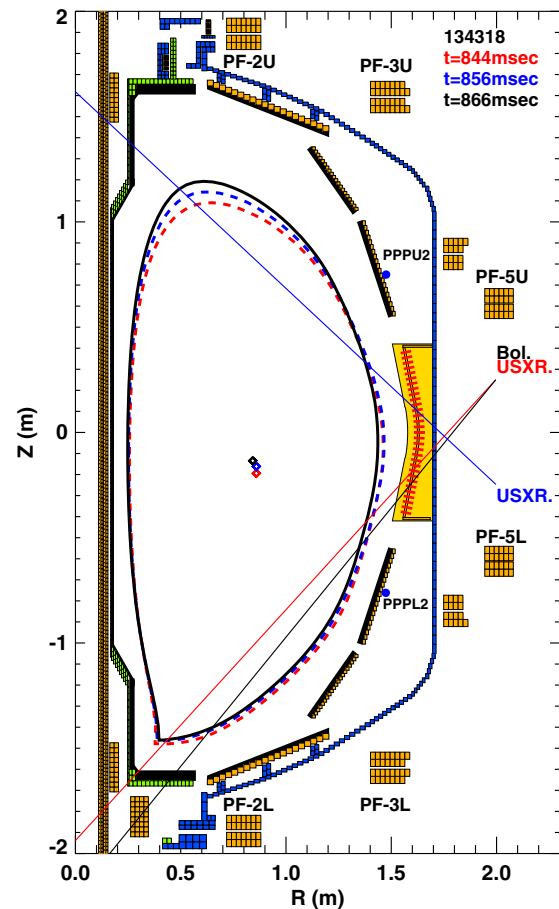

Figure 1. NSTX cross-section, as well as the plasma boundary shape for the 'jogging' plasma at three positions in the motion. Also shown are the coils, the vacuum boundary and graphite plasma facing tiles.

triangularities of about 0.7. The first data set used a plasma current $I_P = 1$ MA, and included the development of the jogging technique in NSTX as well as examples of ELM triggering with 45 Hz vertical jogs. The second data set used discharges with plasma current $I_P = 0.9$ MA and focused on optimizing 30 Hz vertical jogs. The plasmas in this second set were made in the morning following an experiment with significant Li deposition the previous evening, and the residual effects of the Li conditioning, including reduction of ELM activity [49, 50], were clearly present. While small scans of the parameter dr_{sep} (the outboard midplane separation between the magnetic flux lines connected to the upper and lower X-points) were performed on each of the run days, the plasma was always biased towards the lower X-point.

3. Development of jogging techniques

Before these experiments it was not at all clear that the required rapid vertical jogs were achievable in NSTX. The device has a 1.6 cm thick, toroidally continuous stainless steel vessel, which tends to shield the rapid radial-field perturbations that would drive the vertical motion. This is unlike the situation at TCV, where internal coils were used to generate the jogs [35]; external radial coils were used to generate the jogs in ASDEX-Upgrade and JET (note that JET has bellows sections which

increase the toroidal resistance of the vacuum vessel [51]). The techniques used to generate the necessary jogs, and the impact of those jogs on plasma performance, are described below.

The most important coils in this study are the PF-3U and PF-3L coils, labelled in figure 1. These provide four separate functions in NSTX: they control (i) the vertical elongation of the plasma, (ii) the equilibrium vertical location of the magnetic axis (z_{maxis}), (iii) the value of dr_{sep} and (iv) the fast vertical motion of the plasma. Note that double-null configurations have $dr_{sep} \sim 0$, while typical dominantly downward (upward) biased plasma would have $dr_{sep} \sim -1$ to -2 cm (1 to 2 cm). The last three quantities in the above list are controlled, to lowest order, by the value of $I_{PF-3U} - I_{PF-3L}$, which will be referred to as the PF-3 current asymmetry below.

The plasma shape in NSTX is controlled through the combined rtEFIT and isoflux algorithms [52] implemented in the General Atomics Plasma Control System (PCS) [53], originally developed for DIII-D and then implemented on NSTX [47]. Both dr_{sep} and z_{maxis} are available as independent requestable parameters in the shape control algorithm. However, due to the limited number of coils on NSTX (and in particular, the lack of inboard PF coils) dr_{sep} and z_{maxis} are in actuality not independently controllable; for instance, it is not possible to form a lower single null ($dr_{sep} < 0$) shape with the axis above the vessel midplane ($z_{maxis} > 0$). If unrealizable values for these two parameters are requested, the algorithm will find an intermediate shape. For instance, if the requested values are $z_{maxis} = 0$ and $dr_{sep} = -1$ cm, the plasma will be shifted down, but with an achieved dr_{sep} of ≈ -0.5 cm.

There is also a fast vertical position control loop in series with the shape controller [47]. This controller drives a PF-3 current asymmetry that is proportional to the difference in voltages on the flux loops labelled PPPU2 and PPPL2 in figure 1 [47] (the voltages are in turn roughly proportional to the plasma vertical velocity). This fast-feedback is independent of the shape control and always attempts to eliminate plasma vertical motion, though note that it can only respond once the plasma begins to move.

The first attempts at rapidly jogging the plasma utilized short step function downward requests in z_{maxis}. Even with very large (but brief) downward excursion requests, these resulted in rather slow jogs with no noticeable impact on the ELMs. This situation was improved by adding synchronous jogs in dr_{sep}, as shown in figure 2. Frames (*a*) and (*b*) show the synchronous excursions in the requests for z_{maxis} and dr_{sep}. These requests are translated by the control system to the PF-3 asymmetry shown in frame (*c*). The reconstructed oscillating values of dr_{sep} and z_{maxis} are shown in frames (*d*) and (*e*). As expected, dr_{sep} and z_{maxis} oscillate in phase. The reconstructed excursions in both these quantities are significantly smaller than the requests. This is because the plasma does not have sufficient time to respond fully to the (shielded) PF-3 current asymmetry before the shape requests are restored to their pre-jog values, and the PF-3 asymmetry changes sign in order to drive the plasma upwards to its original position.

In the final configuration, it was found that jogs in dr_{sep} alone were sufficient to drive significant motion. Hence, the 30 Hz cases below were conducted with jogs in the dr_{sep} request of between -3 and -5 cm in amplitude and 6 ms in duration.
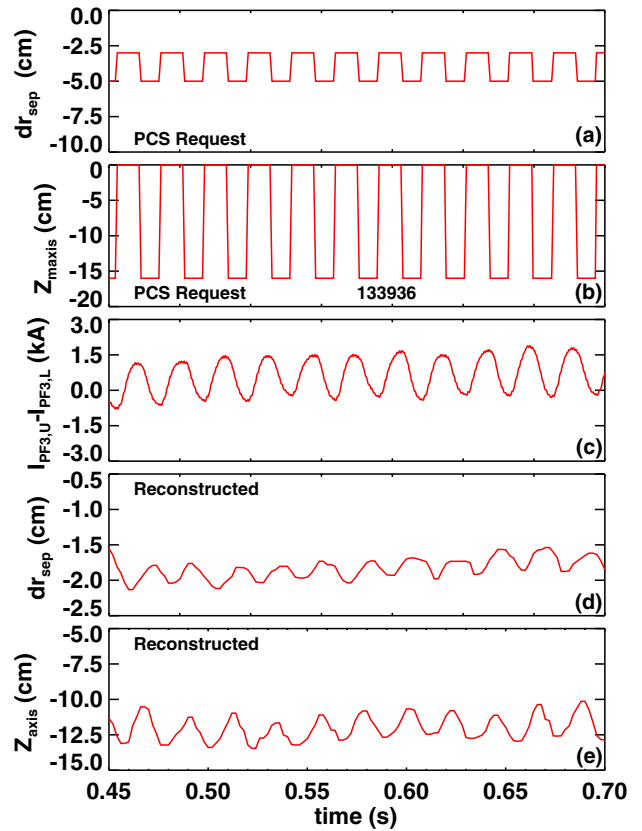

Figure 2. Prescription for generating jogs in NSTX. Shown in (*a*) and (*b*) are the requested dr_{sep} and axis location z_{maxis}. The difference in radial field coil currents is shown in (*c*), while the reconstructed dr_{sep} and axis locations are in (*d*) and (*e*).

However, the 45 Hz jog experiments were conducted before this optimization was complete, and typically have ~ -16 cm jogs in z_{maxis} and -3 cm jogs in dr_{sep}, synchronized and with a duration of ~ 6 ms. Finally, note that while the general prescription described here may work for any tokamak using the isoflux shape control algorithm, the magnitudes and time-scales of the jog requests would depend on factors such as the tokamak conducting structures, control gains and power supply slew rates. These jog-request parameters would need to be developed independently for each facility.

In the analysis below, the reconstructed plasma axis location will be important. It is thus prudent to verify using kinetic measurements that the phase of the vertical motion is correctly calculated. Figure 3(*a*) shows the PF-3 current asymmetry, with the oscillation indicative of the jogs, for a case with jogs but no ELMs (the likely reason for the lack of ELM triggering in this lithium conditioned discharge will be discussed in section 5). The reconstructed axis position is shown in the second frame. The third frame shows the emission from two USXR chords viewing the outer section of the plasma, one chord looking upwards and one chord looking down; because there are no ELMs, the smooth oscillations due to plasma motion are easily observed. The colours of these two traces match those of the viewing chords in figure 1. There are 10 μm Be filters in front of the detectors, so that they are most sensitive to emission from the pedestal region. When the plasma reconstructions indicate upward motion,
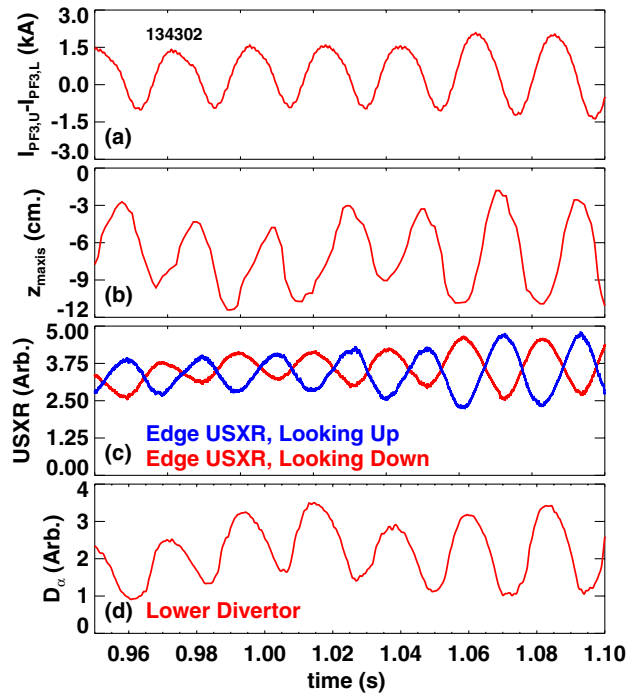
Figure 3. Comparison of the reconstructed jogs with kinetic measurements. Shown are (*a*) the PF-3 coil current asymmetry, (*b*) the reconstructed magnetic axis location, (*c*) the USXR brightness along two chords near the plasma edge and the lower divertor D_α emission.

there is an increase in the signal in the upward viewing USXR chord and a decrease in the downward viewing chord signal; the situation is exactly the opposite when the plasma is reconstructed to be moving down. This is fully consistent with the more hot, and thus bright, plasma farther up the pedestal moving into the sightline of the detector. The lower divertor D_α emission in figure 3(*d*) also shows a reduction in brightness for reconstructed upward motion and an increase in brightness as the plasma moves down. Hence, we infer that the reconstructions are indeed accurately tracking the oscillatory motion. Note, however, that this analysis does not determine whether the amplitude of the reconstructed oscillations is correct.

With this prescription, it was possible to apply large vertical position jogs without deleteriously impacting the plasma performance. In figure 4(*a*) the PF-3 current asymmetry is shown, for two discharges with jogs (30 and 45 Hz), and two reference shots. Figure 4(*b*) shows that the axis vertical position responds to the current asymmetry in the two jogged cases, but is essentially constant in the other two discharges. The normalized β value, a measure of the plasma β normalized to the lowest order scaling [4], $\beta_N = a B_T \beta_T / I_P$, is constant across the four discharges and is at or above the no-wall stability limit. Here β_T is the standard toroidal beta defined in terms of the toriodal magnetic field on axis and the volume average stored energy. For fixed current, field and plasma size, this also implies that the stored energy is unchanged by the jogs. The mid-radius rotation in figure 4(*d*), which is critical for providing passive MHD stability in these high-β conditions [54–56] is similar for all shots. Finally, figures 4(*e*) and (*f*) show the core and pedestal electron and
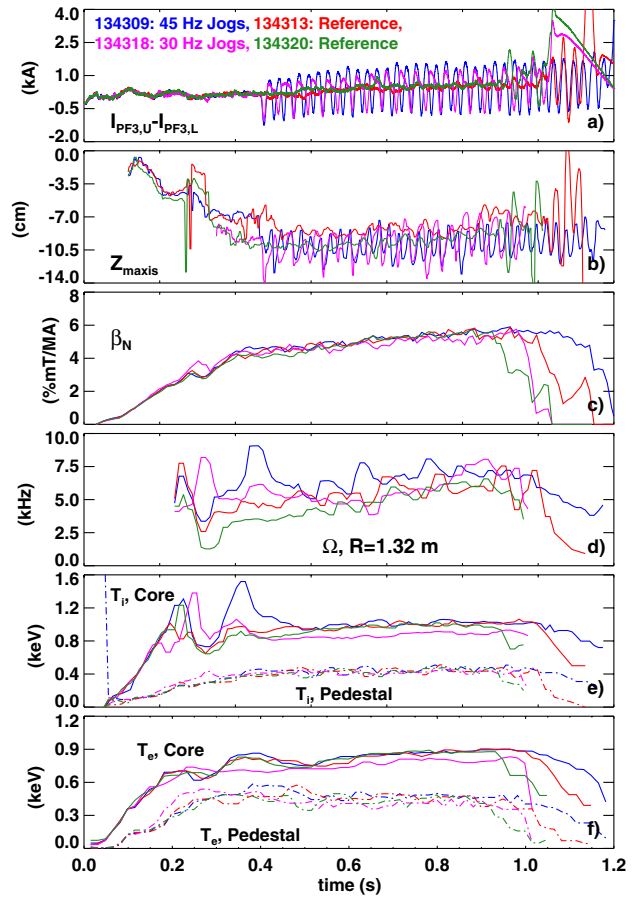

Figure 4. Compatibility of jogging with high-performance operation in NSTX. Shown are (*a*) the difference in radial-field coil currents $I_{PF-3U} - I_{PF-3L}$, (*b*) the axis location z_{maxis}, (*c*) the normalized beta β_N, (*d*) the toroidal rotation frequency Ω at a radius ($R = 1.32$ m) near the $q = 2$ surface, (*e*) the core and pedestal ion temperature and (*f*) the core and pedestal electron temperature.

ion temperatures, where the pedestal temperatures are defined as those at $R = 1.38$ m (near the top of the pedestal in these plasmas). Neither the core nor edge temperatures are deleteriously impacted by the jogs. Note that while ELMs were triggered in the cases with jogs, the timing of the Thomson scattering system was typically not synchronized to the ELMs sufficiently well to resolve the sharp drops; the effect of the ELMs in this case is to add 'noise' to the traces. Also, the 10 ms averaging time in the T_i measurement prevents resolving the effects of the ELMs on the ion temperature.

While it is clear from figure 4 that good performance can be achieved in the presence of careful vertical jogs, it is also possible to drive disruptions with the jogs. These disruptions are not hot-plasma vertical displacement events (VDEs), where control of the plasma vertical position is lost. Unlike, for instance, JET [37, 57] and ASDEX-Upgrade [36], natural ELMs are typically not observed to drive vertical motion in NSTX, and the plasma control system was able to restore the jogged plasma to a centred position in all cases which stayed in H-mode. Indeed, the 4–5 cm jogs are significantly smaller than the maximum recoverable vertical oscillation in NSTX [58]. However, it was observed that when the jog amplitude became either too large or rapid, the plasma position would be driven
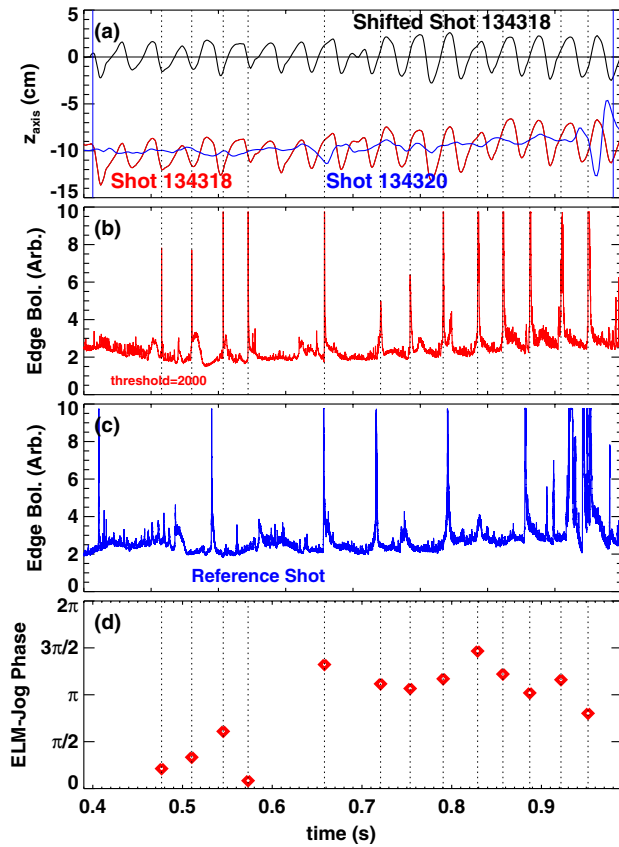
Figure 6. Polar histogram of the ELM-jog phase for 43 ELMs in four discharges with 30 Hz vertical jogs (discharges 134310, 134312, 134314 and 134318).

Figure 5. Observation of ELM pacing in an NSTX plasma with 30 Hz jogs. Shown are (*a*) oscillations in the axis location for the jogged discharge and a reference discharge, ELMs as indicated by the edge bolometer signal for (*b*) the jogged and (*c*) reference shots and (*d*) the ELM-jog phase for each ELM in the time window of interest. The timing of ELMs in the jogged discharge is indicated by vertical dotted lines. The black trace in the upper window is the same at the red one, except that it has been centred on $z = 0$ in order to make the phase relations more clear.

strongly downwards, with insufficient time to recover upwards before the next downward kick. These cases, with average dr_{sep} typically less than -2.5 cm, would lose H-mode, with disruption rapidly following.

4. Observation of ELM pacing and triggering

Clear evidence of type-I ELM pacing with vertical jogs at 30 Hz is demonstrated in figure 5. The upper frame shows the reconstructed magnetic axis location for two shots, one of which has jogs (red) and one of which does not (blue). The discharge without jogs has a slightly more negative equilibrium dr_{sep} request, so that it matches on average the vertical position of the jogged plasma. The reference shot has six ELMs in about 0.5 s, corresponding to a mean frequency of 12 Hz. The jogged shot (134318) has significantly more ELMs; there are 12 large ELMs in the same 0.5 s window, yielding an average frequency of 24 Hz. However, from about $t = 0.65$ s onwards, the ELMs are nearly perfectly frequency matched to the driving waveforms, with the ELM frequency of 30 Hz matching the driving frequency. The boundary shapes at three times during the jogs for this shot are shown in figure 1. It can be seen
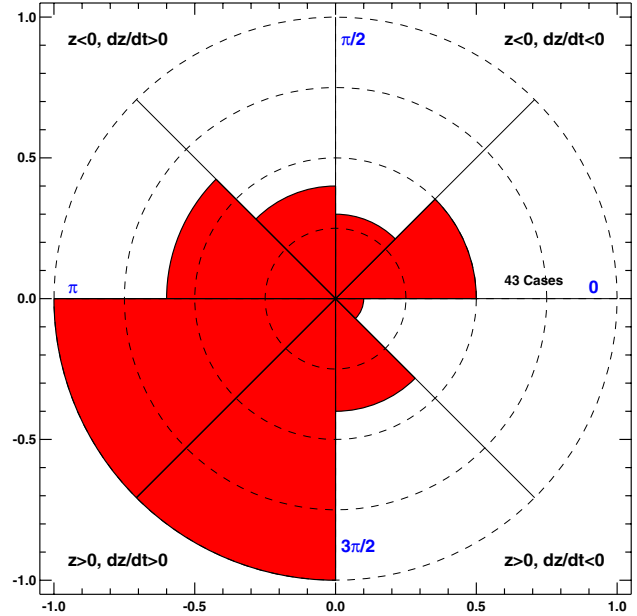
that while the centre of the plasma oscillates by about 4 cm, the plasma top oscillates by more than 10 cm, with the plasma bottom nearly fixed in space.

To more clearly understand the relationship between the driving perturbation and the ELMs, a quantity called the ELM-jog phase is defined. If the ELM occurs when the plasma is centred in its oscillatory motion but moving downwards, the ELM-jog phase is defined to be zero. The phase at the bottom of the motion is then called $\pi/2$, centred but upward moving is π, and the top of the motion is $3\pi/2$. Figure 5(*d*) shows this ELM-jog phase for the chosen jogged discharge. There is an interval at the beginning of the oscillatory phase where ELMs are triggered at the frequency of the jogs, with a phase near $\pi/2$. Then, after a brief delay, the ELMs settle into a pattern with constant frequency and ELM-jog phase between π and $3\pi/2$.

A similar analysis has been done for a sequence of four discharges with 30 Hz jogs, and the ELM-jog phase statistics compiled. The result is shown as a polar histogram in figure 6, where the radius of each wedge is indicative of the number of ELMs in a given bin. This calculation shows that the vast majority of ELMs occur with ELM-jog phase between $\pi/2$ and $3\pi/2$, i.e. when the plasma is moving upwards, away from the divertor coils. This is similar to the result in TCV [35], but is different from the cases in ASDEX-Upgrade [36] and JET [37], where ELMs are observed when the plasma moves downwards.

The results at 30 Hz presented in figures 5 and 6 show clear examples of the ELM cycle driven synchronously with the vertical motion. However, similar studies with 45 Hz jogs have produced less clear synchronization. Figure 7(*a*) shows the axis locations for two similar discharges, one of which has 45 Hz jogs. The ELM activity, as indicated by the edge bolometer, is given in figure 7(*b*). It is clear that the jogging motion results in an increase in the ELM frequency, compared
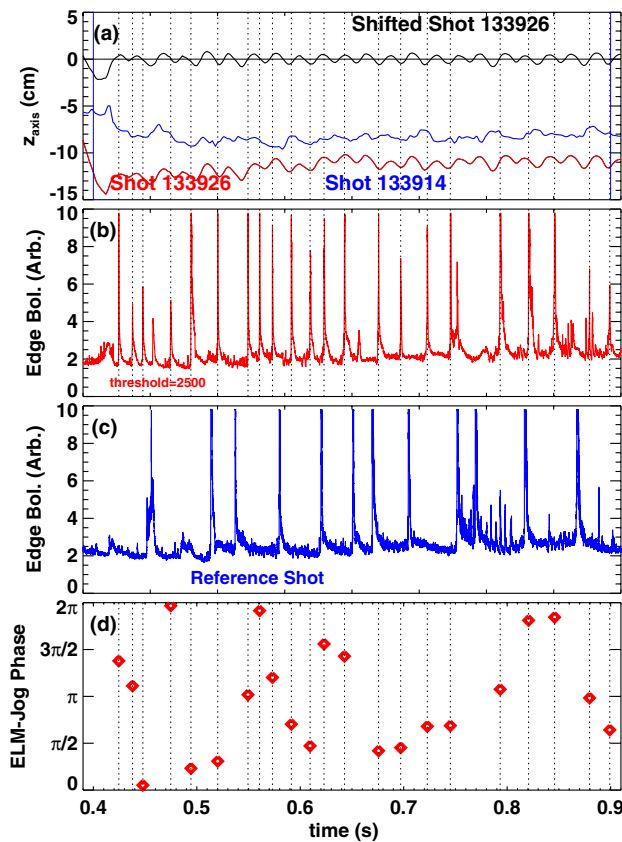
Figure 7. Observation of ELM triggering with 45 Hz jogs. The waveforms are the same as in figure 5.

Figure 8. Fractional ELM sizes versus inverse time between ELMs. The fractional ELM size is defined as the stored energy loss (δW), normalized to the total stored energy before the ELM (W). The shapes of the plot symbols are indicative of the jogging rate.

We can also assess the relative ELM sizes using fast IR-thermography viewing the lower divertor, a new capability for the 2009 NSTX experimental campaign [59]. The data were only available for the cases with 30 Hz jogs. For the reference discharge, the typical ELM lower divertor energy deposition was ∼18 kJ, with a typical frequency of 13 Hz leading to ∼230 kW of power lost through ELMs. For the cases with vertical jogs, the per-ELM power is typically the same, with the increased frequency leading to 2–3 times more power being deposited through ELMs. Note also that the absolute magnitude of the ELM energy loss for these cases is only approximate due to calibration uncertainties associated with changes in the graphite surface emissivity after lithium evaporation.

5. Discussion, conclusions and future work

A number of explanations have been put forth in the past to explain the triggering of ELMs via vertical position jogs. In TCV, it was observed that ELMs were triggered as the plasma moved away from the divertor coil. Given that this direction of motion initiates an increase in the edge-current density [60], it leads to the plausible explanation that an increase in the edge current creates the ELMs. This explanation was called into question, however, by the ASDEX-Upgrade results, where downward motion (towards the divertor coil) triggered ELMs [36]; the situation in JET is apparently similar to that in ASDEX-Upgrade [37]. These results suggest that the edge-current perturbations were not solely responsible for the ELM triggering.

The time varying equilibrium properties of jogged ASDEX-Upgrade and TCV plasmas were studied by Kim *et al* [60]. In addition to clarifying the evolution of the current profile during the jogs, that work indicated other potential destabilizing mechanisms. For instance, an expansion of the plasma surface in the upper outer quadrant was observed in both devices, which had a tendency to destabilize the edge in free-boundary stability calculations. However, the warning was given that considering the variety of ELM types and complicated nature of ELM stability, and the many different equilibrium properties that change during the jogs, it may not

with the reference shot in figure 7(*c*)). However, as indicated by the ELM-jog phase in figure 7(*d*)), the resulting ELMs are not strongly correlated with any particular phase of the jogging motion. This result was reproducible for a number of 45 Hz jog discharges and reference shots; the jogs accelerated the ELM frequency, but the ELMs were not clearly synchronized to any given phase of the vertical motion.

The ELM size, as defined by the immediate reduction in stored energy following the ELM, is a key parameter in studying the utility of any ELM pacing technique. For uniform analysis of all discharges in the dataset, this energy loss (δW) was measured using the change in diamagnetic flux following an ELM. The results of the analysis are shown in figure 8. The frequency associated with any given ELM is defined as the inverse time between that ELM and the one immediately preceding it. There is significant scatter among the frequencies, resulting from the lack of clear synchronization at 45 Hz and jogs without ELMs at 30 Hz. However, a clumping of (red) points at approximately 30 Hz can be observed, corresponding to the synchronized and paced ELMs in figures 5 and 6. The cases with no jogs and with 30 Hz jogs tend to have ELMs of about the same size; no beneficial reduction in the ELM size is observed in this case. For the ELMs initiated by 45 Hz jogs, the more rapid ELMs result in a significant reduction in the typical ELM size. Hence, while the physics behind the destabilization for this rapid jog case remains obscure, the resulting ELM characteristics were improved.
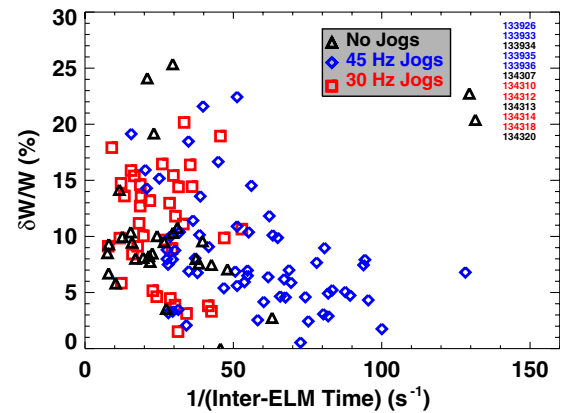
be possible to find a single explanation that fits all devices and examples.

The results presented here tend to confirm this notion of multiple interacting effects leading to the ELM pacing. The large type-I ELMs are, at least for the 30 Hz case, triggered preferentially during the upward motion. This would be consistent with an explanation in line with that from TCV, where the increased edge current leads to destabilization. This line of reasoning is further supported by the observation presented in [50]: at the low aspect ratio and strong shaping in NSTX, the edge-current (peeling) boundary is typically that which is crossed to precipitate an ELM. This explanation is also consistent with the observation that, for fixed jog amplitude, ELMs were more difficult to trigger immediately following a heavy lithiumization. It has been shown [50] in similar plasmas that the peeling mode boundary moves to larger edge-current density with lithium conditioning, leading to an elimination of ELM activity; this shift in the stability boundary would then mandate larger edge-current perturbations in order to cross the instability threshold. Indeed, in the present experiments, the lithium conditioning proceeding the second experimental day drove the decision to reduce the jog frequency to 30 Hz (from 45 Hz), leading to an increase in the fraction of jogs that triggered ELMs.

This edge-current based explanation, however, cannot be simply reconciled with the observed lack of synchronization between jogs and ELMs in the 45 Hz case. Hence, the understanding of the physics underlying the triggering remains incomplete.

The initial results presented here show that there is considerable future work to do on this subject. The overarching goal of these studies is to increase the ELM frequency, so as to reduce the ELM size; from figure 8, it appears that ~60 Hz (or faster) ELMs are a reasonable goal for NSTX; no effort was made in these experiments to trigger at this rate, and so it remains unclear what the maximum frequency actually is. Next steps under consideration include testing the jogs at triangularities closer to those in the other experiments, and exploring more explicitly the dr_{sep} dependence of the ease of pacing. We will also explore the ability of 3D fields to reduce the jogging amplitude required for achieving ELMs, and to increase the reliability of the triggering.

In summary, scenarios for ELM pacing via rapid vertical jogs have been developed for the first time in a ST plasma. Large step requests in the parameters z_{maxis} or dr_{sep} are used to force rapid plasma oscillations. When the frequencies of these jogs are set to 30 Hz, synchronization of the ELM cycle with the jogs has been observed. With 45 Hz jogs, the ELMs were observed to become quite rapid, though the synchronization to the plasma motion was unclear. These rapid ELMs resulted in a substantial reduction in the per-ELM energy loss, and thus indicate a desired path forward for future studies.

Acknowledgments

References

[1] Wagner F. *et al* 1982 *Phys. Rev. Lett.* **49** 1408
[2] Dimits A.M. *et al* 2000 *Phys. Plasmas* **7** 969
[3] Menard J.E., Jardin S.C., Kaye S.M., Kessel C.E. and Manickam J. 1997 *Nucl. Fusion* **37** 595
[4] Strait E.J. 1994 *Phys. Plasmas* **1** 1415
[5] Galeev A.A. 1971 *Sov. Phys.—JETP* **32** 752
[6] Zarnstorff M.C. and Prager S.C. 1984 *Phys. Rev. Lett.* **53** 454
[7] Peeters A.G. 2000 *Plasma Phys. Control. Fusion* **42** B231
[8] Zohm H., Ryter F., Fuchs C., Herrmann A., Kaufmann M., Neuhauser J. and Salmon N. 1994 *Plasma Phys. Control. Fusion* **36** A129
[9] Connor J.W. 1998 *Plasma Phys. Control Fusion* **40** 531
[10] Bécoulet M. *et al* and Contributors to JET-EFDA Workprogramme 2003 *Plasma Phys. Control. Fusion* **45** A93
[11] Kamiya K. *et al* 2007 *Plasma Phys. Control. Fusion* **49** S43
[12] Connor J.W. 1998 *Plasma Phys. Control Fusion* **40** 191
[13] Snyder P.B., Wilson H.R., Ferron J.R., Lao L.L., Leonard A.W., Osborne T.H., Turnbull A.D., Mossessian D., Murakami M. and Xu X.Q. 2002 *Phys. Plasmas* **9** 2037
[14] Federici G., Loarte A. and Strohmayer G. 2003 *Plasma Phys. Control Fusion* **45** 1523
[15] Federici G. 2006 *Phys. Scr.* **T124** 1
[16] Loarte A. *et al* and the ITPA Scrape-off Layer and Divertor Physics Topical Group 2007 Progress in the ITER Physics Basis Chapter 4: Power and Particle Control *Nucl. Fusion* **47** S203
[17] Hawryluk R.J. *et al* 2009 *Nucl. Fusion* **49** 065012
[18] Evans T.E. *et al* 2006 *Nature Phys.* **2** 419
[19] Fenstermacher M.E., Evans T.E., Osborne T.H., Schaffer M.J., deGrassie J.S., Gohil P., Moyer R.A. and the DIII-D Team 2008 *Nucl. Fusion* **48** 122001
[20] Evans T.E. *et al* 2008 *Nucl. Fusion* **48** 024002
[21] Burrell K.H. *et al* 2005 *Phys. Plasmas* **12** 056121
[22] Burrell K.H., Osborne T.H., Snyder P.B., West W.P., Fenstermacher M.E., Groebner R.J., Gohil P., Leonard A.W. and Solomon W.M. 2009 *Nucl. Fusion* **49** 085024
[23] Suttrop W. *et al* and the ASDEX Upgrade Team 2003 *Plasma Phys. Control. Fusion* **45** 1399
[24] Suttrop W. *et al*, the ASDEX Upgrade team and contributors to the JET-EFDA workprogramme 2005 *Nucl. Fusion* **45** 721
[25] Sakamoto Y., Shirai H., Fujita T., Ide S., Takizuka T., Oyama N. and Kamada Y. 2004 *Plasma Phys. Control. Fusion* **46** A299
[26] Takase Y. *et al* 1997 *Phys. Plasmas* **4** 1647
[27] Kaye S.M. *et al* 1984 *J. Nucl. Mater.* **121** 115
[28] Doyle E.J., Groebner R.J., Burrell K.H., Gohil P., Lehecka T., Luhmann N.C. Jr, Matsumoto H., Osborne T.H., Peebles W.A. and Philipona R. 1991 *Phys. Fluids B* **3** 2300
[29] Maingi R. *et al* 2005 *Nucl. Fusion* **45** 264
[30] Lang P.T. *et al* and the ASDEX Upgrade Team 2004 *Nucl. Fusion* **44** 665
[31] Lang P.T. *et al*, the ASDEX Upgrade Team and JET-EFDA contributors 2008 *Nucl. Fusion* **48** 095007
[32] Lang P.T., Alper B., Buttery R., Gal K., Hobirk J., Neuhauser J., Stamp M. and JET-EFDA contributors 2007 *Nucl. Fusion* **47** 754
[33] Canik J.M. *et al* and the NSTX Team 2010 *Phys. Rev. Lett.* **104** 045001
[34] Gates D.A. *et al* 2009 *Nucl. Fusion* **49** 104016
[35] Degeling A.W., Martin Y.R., Lister J.B., Villard L., Dokouka V.N., Lukash V.E. and Khayrutdinov R.R. 2003 *Plasma Phys. Control Fusion* **45** 1637
[36] Lang P.T. *et al* and ASDEX Upgrade Team 2004 *Plasma Phys. Control. Fusion* **46** L31
[37] Sartori F., Lomas P., Piccolo F., Zedda M.K. and JET EFDA contributors 2008 Synchronous ELM pacing at JET using the vertical stabilization controller *35th EPS Conf. on*

Plasma Physics (Hersonissos, Crete, Greece)
http://eps2008.iesl.forth.gr/index.html

[38] Romanelli F. *et al* and JET-EFDA, Culham Science Centre, Abingdon, Oxfordshire OX14 3DB, UK JET-EFDA Contributors 2009 *Fusion Eng. Des.* **84** 150

[39] de la Luna E. 2009 ELM mitigation studies in JET and implications for ITER *APS–DPP Meeting (Atlanta, USA, 2009)* PI2.00002 see http://meetings.aps.org/Meeting/DPP09/Event/109696

[40] Snyder P.B., Wilson H.R., Osborne T.H. and Leonard A.W. 2004 *Plasma Phys. Control. Fusion* **46** A131

[41] Ono M. *et al* and the NSTX Team 2000 *Nucl. Fusion* **40** 557

[42] Peng Y.K.M. and Strickler D.J. 1986 *Nucl. Fusion* **26** 769

[43] Maingi R. *et al* 2003 *Nucl. Fusion* **43** 969

[44] Maingi R. *et al* and the NSTX Team 2004 *Plasma Phys. Control. Fusion* **46** A305

[45] Maingi R. *et al* 2005 *Nucl. Fusion* **45** 1066

[46] Maingi R. *et al* 2005 *J. Nucl. Mater.* **337–339** 727

[47] Gates D. *et al* 2006 *Nucl. Fusion* **46** 17

[48] Stutman D., Finkenthal M., Soukhanovskii V., May M.J., Moos H.W. and Kaita R. 1999 *Rev. Sci. Instrum.* **70** 572

[49] Mansfield D.K. *et al* 2009 *J. Nucl. Matter* **390–391** 764

[50] Maingi R *et al* and the NSTX Research Team 2009 *Phys. Rev. Lett.* **103** 075001

[51] Huguet M., Dietz K., Hemmerich J.L. and Last J.R. 1987 *Fusion Technol.* **11** 43

[52] Ferron J.R., Walker M.L., Lao L.L., St. John H.E., Humphreys D.A. and Leuer J.A. 1998 *Nucl. Fusion* **38** 1055

[53] Ferron J.R., Kellman A.G., McKee G.R., Osborne T.H., Petrach P., Taylor T.S. and Wight J. 1992 An advanced plasma control system for the DIII-D tokamak *Proc. 14th IEEE/NPSS Symp. on Fusion Engineering, San Diego, USA* vol II p 761

[54] Sontag A.C. *et al* 2005 *Phys. Plasmas* **12** 056112

[55] Sabbagh S.A. *et al* 2006 *Nucl. Fusion* **46** 635

[56] Gerhardt S.P. *et al* 2009 *Nucl. Fusion* **49** 032003

[57] Villone F., Riccardo V., Sartori F. and Contributors to the EFDA-JET workprogramme 2005 *Nucl. Fusion* **45** 1328

[58] Humphreys D.A. *et al* 2009 *Nucl. Fusion* **49** 115003

[59] Ahn J.-W., Maingi R., Mastrovito D. and Roquemore A.L. 2010 *Rev. Sci. Instrum.* **81** 023501

[60] Kim S.H. *et al* 2009 *Plasma Phys. Control. Fusion* **51** 055021

The Princeton Plasma Physics Laboratory is operated
by Princeton University under contract
with the U.S. Department of Energy.

Information Services
Princeton Plasma Physics Laboratory
P.O. Box 451
Princeton, NJ 08543

Phone: 609-243-2245
Fax: 609-243-2751
e-mail: pppl_info@pppl.gov
Internet Address: http://www.pppl.gov